Eur. Phys. J. B **29**, 547–552 (2002)
DOI: 10.1140/epjb/e2002-00338-y

THE EUROPEAN PHYSICAL JOURNAL B

Magnetization and neutron scattering studies of the pressure effect on the magnetic transition in $Er_{0.57}Y_{0.43}Co_2$

A. Podlesnyak[1,2,a], Th. Strässle[1], A. Mirmelstein[2], A. Pirogov[2], and R. Sadykov[3]

[1] Laboratory for Neutron Scattering, ETH Zürich & Paul Scherrer Institut, 5232 Villigen PSI, Switzerland
[2] Institute for Metal Physics RAS, 620219 Ekaterinburg GSP-170, Russia
[3] Vereshchagin High-Pressure Physics Institute RAS, 142092 Troitsk, Moscow region, Russia

Received 20 December 2001 / Received in final form 12 June 2002
Published online 31 October 2002 –

Abstract. Neutron powder diffraction was employed to study the pressure effect on the magnetic transition in the pseudobinary Laves-phase compound $Er_{0.57}Y_{0.43}Co_2$ and to determine the magnetic moments of the Er- and Co-subsystems. Our studies reveal that the onset of long-range magnetic order for both the localized $4f$ (Er) and itinerant $3d$ (Co) electron moments appears at about the same temperature at ambient pressure. The pressure effect on T_c is found to be negative and equal for both sublattices, namely $\partial T_c/\partial \mathrm{p} \sim -0.4$ K/kbar. The values of the magnetic moments of the Er and the Co ions are found $\mu_{\mathrm{Er}} = 5.40 \pm 0.15\mu_B$/atom, $\mu_{\mathrm{Co}} = 0.50 \pm 0.07\mu_B$/atom and $5.35 \pm 0.15\mu_B$/atom, $0.37 \pm 0.09\mu_B$/atom, for $p = 0$ and 6 kbar, respectively. Our experimental results give evidence for short-range magnetic order formation at temperatures already above T_c and for a coexistence short- and long-range order below T_c down to 4 K.

PACS. 75.30.Kz Magnetic phase boundaries (including magnetic transitions, metamagnetism, etc.) – 75.25.+z Spin arrangements in magnetically ordered materials (including neutron and spin-polarized electron studies, synchrotron-source X-ray scattering, etc.) – 74.62.Fj Pressure effects – 61.12.-q Neutron diffraction and scattering

1 Introduction

Since itinerant electron metamagnetism (IEM) was first predicted by Wohlfarth and Rhodes [1], the pseudobinary Laves-phase compounds $R_{1-x}Y_xCo_2$ (R = magnetic rare-earth) were subject of extensive studies (see *e.g.* [2] and references therein). In particular, much attention was paid to the limited range around the critical Y concentration x_c at which the intersublattice molecular field H_{fd}^{Co}, provided by the rare-earth moments, becomes equal to the critical field of the metamagnetic transition H_{cr}. The temperature and composition dependences of the transport properties, magnetization, magnetic anisotropy and magnetostriction of $R_{1-x}Y_xCo_2$ in varying external conditions (T, H, p) have been extensively studied by numerous research groups [3–10]. In particular, it was shown that x_c depends on the type of R ion [10]. Nakamura pointed out that a large magnetovolume effect observed in these compounds is attributed to the Co moment induced by H_{fd}^{Co} [11]. By means of neutron diffraction and susceptibility measurements Baranov *et al.* found a coexistence of short- and long-range magnetic order within a narrow concentration range near x_c [4–6]. The effect of pressure on the itinerant $3d$ electron subsystem was first discussed by Yamada and Shimizu [15] and later considered by Yamada in the frame of the phenomenological Landau-Ginzburg theory [16]. Taking into account spin fluctuations he concluded that H_{cr} increases with increasing pressure and consequently the metamagnetic transition should be suppressed above a critical pressure p_{cr}. Spin fluctuations have been shown to give dominant contributions to the metamagnetic properties at finite temperature and also to their pressure dependences *via* the volume magnetostriction.

It should be noted, that the authors of the above mentioned papers discussed the magnetic behavior of these pseudobinary $R_{1-x}Y_xCo_2$ systems assuming a single magnetic transition temperature T_c for both the R and Co magnetic sublattices. Recently, Hauser *et al.* suggested that in a limited concentration range $x_{cr'} < x < x_{cr}$ and pressure $p_{cr'} < p < p_{cr}$ there is a decoupling of the magnetic order of the rare-earth and the Co sublattice [12–14]. In other words, in $Er_{1-x}Y_xCo_2$ the itinerant Co sublattice orders at a lower temperature than the Er sublattice. This is explained by a weakening of the effective molecular field H_{fd}^{Co} acting on the Co sites due to the yttrium

[a] e-mail: andrew.podlesnyak@psi.ch

substitution or due to a pressure-driven increase of the critical field necessary to induce a magnetic moment on the Co sites.

The experimental information concerning the pressure effect on the IEM are very limited. Measurements of the electrical resistivity and magnetic susceptibility in $Er_{1-x}Y_xCo_2$ were carried out by Hauser *et al.* (using a Bridgman cell, $p < 60$ kbar, $0 < x < 0.5$) [14,17] and by Syshchenko *et al.* (using a cubic-anvil device, $p < 80$ kbar, $x = 0$) [18,19]. It was found that at lower pressures ($p < 20$ kbar) T_c decreases linearly with increasing pressure. At higher pressures, the T_c *vs.* p dependence strongly deviates from linearity and above a critical pressure $p_{cr} \sim 40$ kbar the T_c becomes nearly pressure independent [18]. Hauser *et al.* suggested that the decoupling of the magnetic ordering transition temperature found for the Y diluted compounds rapidly increases with pressure, and consequently above $p_{cr}(x)$ only the Er sublattice exhibits long-range ordering. Note, that the T_c value for the $ErCo_2$ ($\sim$13 K at $p > 40$ kbar) reported in [18] is significantly lower in contradiction to the $T_c = 22$ K published in [14].

Surprisingly, very few data on the magnetic behavior in $R_{1-x}Y_xCo_2$ by means of neutron scattering have been published so far. To our knowledge there is no neutron diffraction data about the IEM under external pressure in the current literature. In many cases the determination of the magnetization by neutron diffraction techniques is invaluable in the interpretation of bulk phenomena. In this paper we report the results of the magnetic and neutron diffraction measurements on $Er_{0.57}Y_{0.43}Co_2$ under pressure which were undertaken to clarify the behavior of the magnetic Er- and Co-subsystems near the critical concentration x_c.

2 Experiment

The $Er_{0.57}Y_{0.43}Co_2$ compound was prepared by arc melting under helium atmosphere followed by homogenization at 1220 K for 50 hours. X-ray investigation of the sample revealed the cubic $MgCu_2$ structure type as expected (space group Fd3m). The content of impurity phases (mainly $ErCo_3$) was less than 3%.

The neutron diffraction experiments were carried out using a zero-matrix clamp pressure cell. The axially symmetric cell made of Zi/Ti alloy with an inner diameter of 7.5 mm allowed a total sample volume of about 1900 mm^3. Fluorinert FC-77 was used as a pressure medium. The pressure was determined by the shift in the lattice parameter of NaCl added to the sample [20]. The data were collected on the HRPT high-resolution diffractometer [21] at the spallation source SINQ, Switzerland, using a wavelength of $\lambda = 1.886$ Å. A standard orange ILL cryostat was used in the temperature range between 4 and 40 K. For the refinement of the magnetic structure the program FullProf was applied [22].

The measurements of the magnetic susceptibility were carried out on a Quantum Design PPMS system. For the experiments under pressure a clamp cell made of non-magnetic Cu/Be alloy was used allowing pressures up to 10 kbar. Within the cell the powder sample was placed in a very thin capsule made of lead and filled with Fluorinert FC-77. The superconducting transition temperature of the lead was used to measure the pressure [23].

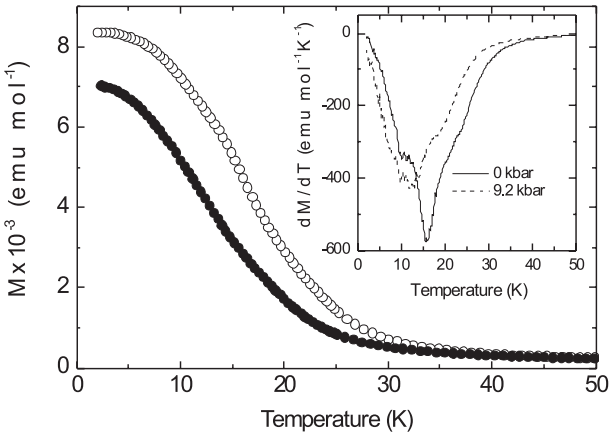

Fig. 1. Temperature dependence of the FC magnetization $M(T)$ of the $Er_{0.57}Y_{0.43}Co_2$ in an external field of 0.1 T. Open and solid symbols denote measurements at zero pressure and $p = 9.2$ kbar, respectively. The inset shows the pressure-dependent shift of of the dM/dT curve.

3 Results

3.1 Magnetic measurements

Macroscopic measurements under pressure have been widely described recently [12,17–19]. Here, we only report on the temperature dependence of the magnetization $M(T)$ of the $Er_{0.57}Y_{0.43}Co_2$ compound at ambient pressure as well as $p = 9.2(2)$ kbar. It should be noted that we have chosen this particular composition, since according to a previous study [4] $x = 0.43$ is close to the critical concentration $x_c \sim 0.45$ for the $Er_{1-x}Y_xCo_2$ compound andlarge pressure effects are expected.

The M *vs.* T curves for a field-cooled (FC) regime at a low magnetic field of 0.1 T were measured. As one can see from Figure 1 the magnetization curves show ferromagnetic behavior with smooth magnetization changes around T_c typical for second order transitions. The Curie temperatures were associated with the minima in the dM/dT curves (see inset in Fig. 1), $T_c(0 \text{ kbar}) = 16 \pm 0.5$ K and $T_c(9.2\text{kbar}) = 12 \pm 0.5$ K. The deduced value $\partial T_c/\partial p$ of -0.43 K/kbar is in good agreement with literature data [14].

3.2 Neutron powder diffraction

The neutron diffraction patterns of $Er_{0.57}Y_{0.43}Co_2$ recorded below the respective Curie temperatures at $p = 0$ and 6.0(5) kbar show only a variation in the intensity of

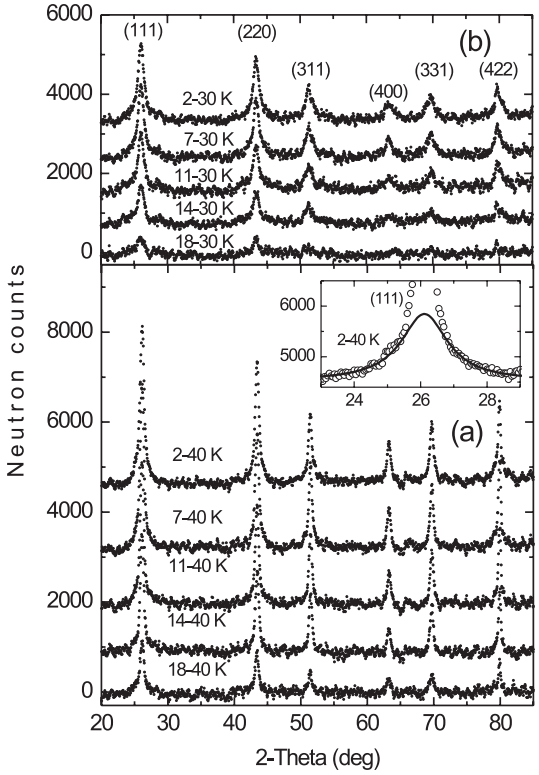

Fig. 2. Evolution of the magnetic scattering with temperature in the $Er_{0.57}Y_{0.43}Co_2$ compound at zero pressure (a) and at $p = 6$ kbar (b). Miller indices of magnetic reflections used for the refinement are noted. The inset shows the diffuse scattering near the (111) reflection. The solid line represents the result of a fit to the Lorentzian line-shape.

the nuclear reflections without the appearance of additional lines. Thus, in the magnetically ordered state the magnetic contribution obtained, corresponds to a collinear alignment of the magnetic moments of the Er and Co ions (μ_{Er} and μ_{Co}, respectively). The observed neutron magnetic patterns, which were obtained as the difference of the intensities below and above T_c, are summarized in Figure 2. The intensities of the reflections increase with decreasing temperature indicative for the growing Er and Co sublattice moments. The neutron magnetic diffraction patterns exhibit a pronounced diffuse magnetic scattering around the nuclear Bragg reflections (see inset in Fig. 2) which indicates the presence of short-range order of the Er- and Co-subsystem.

4 Analysis and discussion

Figure 3 shows the temperature dependences of the lattice parameter a in the $Er_{0.57}Y_{0.43}Co_2$ compound obtained from the neutron diffraction measurements. The importance of the lattice constant of RCo_2 compounds in the vicinity of an IEM has been recently demonstrated by Khmelevskyi and Mohn [24] by fixed-spin-moment band-structure calculations. They deduced that an IEM

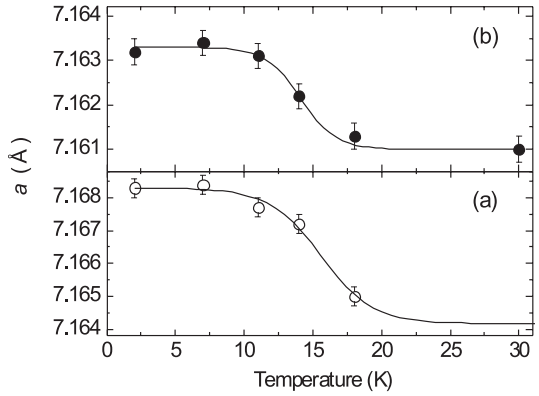

Fig. 3. The temperature dependence of the lattice parameter of the $Er_{0.57}Y_{0.43}Co_2$ compound at ambient pressure (a) and $p = 6$ kbar (b). The solid lines are fits on the sigmoidal function according to equation (1).

transition can occur only over a certain range of lattice constants and that the possibility of a first order phase transition is connected to features of the electronic structure rather than to the magnitude of the transition temperature as conjectured earlier. As we mentioned in the introduction the jump-like lattice expansion is directly attributed to the positive magnetovolume effect accompanying the long-range ordering of the itinerant $3d$ Co electron moments, $\Delta V/V \sim k\mu_{Co}^2$, where k is the magnetovolume coupling constant. In pure $ErCo_2$ this anomaly $\Delta V/V$ reaches 4.5×10^{-3} [8], whereas it is significantly reduced in the case of diluted $Er_{1-x}Y_xCo_2$ (Fig. 3). The pressure-induced decrease of interatomic distances leads to a broadening of the Co-$3d$ band and, consequently to a decrease of the Co-$3d$ density of states in the vicinity of E_f. The values $\Delta V/V$ obtained from our neutron diffraction data turn out to be 5.7×10^{-4} and 3.2×10^{-4} for $p = 0$ and 6 kbar, respectively. The fact that we observe a small but pronounced volume expansion confirms a Co moment formation at $x_c \sim 0.43$. Supposing that k does not change substantially, we directly deduce that μ_{Co} decreases with pressure.

We observed diffuse magnetic scattering around the nuclear Bragg reflections, which is formed already slightly above T_c and exists down to low temperatures (Fig. 2). This supports a model of the magnetic state in which the long-range magnetic ordering coexists with short-range correlations due to statistical effects of the Co-Y and Co-Er local environment [6,7]. This is also confirmed by the results of electrical resistivity and heat capacity measurements [3,5,17]. The residual resistivity ρ and the coefficient γ of the linear term of the low-temperature specific heat of $R_{1-x}Y_xCo_2$ were found to be very high for $x \sim x_c$ compared to pure $ErCo_2$ and to be irreversibly decreased by an applied magnetic field [5]. The NMR investigations of the itinerant paramagnets $Lu(Co_{0.92}Al_{0.08})_2$ have also shown a coexistence of non-magnetic and magnetic ($\mu_{Co} \sim 0.65\mu_B$) states of the Co-ions [25].

It is important to stress, that the observed magnetic peaks do not overlap (Fig. 2). Moreover, to establish the

Table 1. Observed magnetic integrated intensities I_{obs} after diffuse scattering correction (described in the text), and calculated intensities I_{cal} from the best fit using the integrated intensities mode of the FullProf program. Upper and lower parts of the table correspond to the measurements at zero pressure and $p = 6$ kbar, respectively.

hkl	111		220		311		400		331		422	
T, K	I_{obs}	I_{cal}	I_{obs}	I_{cal}	I_{obs}	I_{cal}	I_{obs}	I_{cal}	I_{obs}	I_{cal}	I_{obs}	I_{cal}
2	2954	3056	2038	2168	1162	1180	628	569	887	844	995	966
7	2774	2835	1836	1965	1002	991	590	547	824	800	897	869
11	2344	2398	1490	1540	978	953	500	442	689	696	728	671
14	1890	1816	1299	1395	869	831	402	377	567	532	634	580
18	875	878	560	615	347	314	186	160	258	285	274	207
2	2461	2499	1864	1896	956	968	520	503	757	723	910	906
7	2425	2380	1789	1808	913	906	513	471	741	708	874	889
11	1866	1882	1501	1467	821	804	393	354	583	568	734	843
14	1096	1149	892	914	504	475	213	143	344	314	436	475
18	406	496	320	377	175	147	65	42	87	30	156	180

temperature dependence of μ_{Co} and μ_{Er} we are interested mostly in relative magnetic intensity changes. Under these circumstances, the refinement with FullProf program in the integrated intensities mode should be most preferable, as is explained in [22]. Thus, to determine the long-range ordered magnetic moments μ_{Co} and μ_{Er} we first subtracted the diffuse scattering (approximated by a Lorentzian following [6], see inset in Fig. 2a) from the observed neutron magnetic scattering. We then numerically integrated the Bragg magnetic reflections to avoid an error due to line-shape fitting. These integrated intensities were used in the refinement of the magnetic moments of the Er and Co sublattices. The scale factor was obtained from the refinement of the diffraction pattern in the paramagnetic state. The observed and calculated magnetic integrated intensities are summarized in Table 1. The calculated temperature dependences of the Er and Co magnetic moments are presented in Figure 4. It is seen that the pressure effect on T_c is negative. The Co magnetic moment decreases with pressure (in agreement with the above mentioned decrease of the magnetovolume effect), unlike μ_{Er}, which seems to be stable. Note that the μ_{Er} turns out to be constant at the metamagnetic transition in pure $ErCo_2$ as well [26].

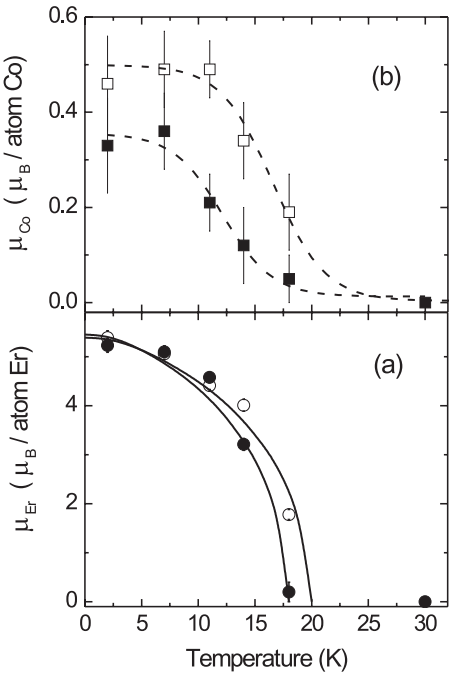

Fig. 4. The temperature dependences of the magnetic moments of the Er (a) and Co (b) sublattices at zero pressure (open symbols) and $p = 6$ kbar (filled symbols). The dashed and solid lines represent the fitted magnetization curves derived from equations (1, 2), respectively (see text).

There are six different types of structure factors in the cubic Laves-phase, depending on the values of h, k and l. It is noteworthy to mention that two of them are characteristic of the Er atoms only (h or k or $l \neq 4n$ and $h+k+l = 4n$) or of the Co atoms only (h, k and $l = 4n+2$). However in our diffraction patterns the (222) peak, specific for the Co, turned out to be inaccessible due to constraints given by the pressure cell. Nevertheless the fit yielded a well determined magnetic moment μ_{Co}. For instance, the refinement at $T = 14$ K and $p = 0$ kbar leads to a final $R_f = 6.33$ and $\chi^2 = 0.48$ with Er and Co moments of $\mu_{\mathrm{Er}} = 4.0(1)\ \mu_B$/atom Er and $\mu_{\mathrm{Co}} = 0.34(8)\mu_B$/atom Co, respectively (see Fig. 4). In the best fit, with the Co assumed to carry no moment, we obtained $R_f = 16.7$ and $\chi^2 = 3.37$. This example shows that the result is sensitive to the presence of even small magnetic moments at the Co site.

In order to compare the temperature and pressure dependences of the Er and Co magnetic sublattices both $\mu_{\mathrm{Co}}(T)$ and $a(T)$ may be approximated by a sigmoidal function:

$$y = \frac{y_{max} - y_{min}}{1 + \exp\left\{\frac{T - T_0}{\Delta T}\right\}} + y_{min}, \qquad (1)$$

Table 2. Characteristic values of the magnetic transitions derived from the temperature dependences of the lattice parameter a [Å] (I and II) and magnetic moment $\mu_{\rm Co}$ [μ_B/atom] (III and IV) using equation (1).

	I	II	III	IV
p, kbar	0	6.0(5)	0	6.0(5)
y_{min}	7.1642(3)	7.1610(3)	0	0
y_{max}	7.1683(3)	7.1633(3)	0.50(7)	0.37(9)
T_0, K	15.6(7)	14.1(7)	16.6(9)	12.0(9)
ΔT, K	1.8(5)	1.3(9)	2.3(5)	2.7(8)

with T_0 and ΔT a measure for the phase transition temperature and the width of the transition, respectively.

The magnetization of the rare-earth subsystem $\mu_{\rm Er}(T)$ can be expressed in the molecular-field approach [2] by the Brillouin function B_J:

$$\mu_R = g_R J_R \mu_B B_J \left[\frac{g_R J_R \mu_B}{kT} H_{fd}^R \right], \qquad (2)$$

where g_R is the g factor, J_R is the total quantum number of the rare earth and with H_{fd}^R the molecular field being the only fitting parameter.

The results of the fits are shown in Figures 3, 4 and are summarized in the Table 2. It is seen that the Er sublattice magnetization is changing in a wider temperature interval than the Co sublattice which is reflected in $\mu_{\rm Co}(T)$ and $a(T)$.

Table 3 summarizes the characteristic temperatures T_c of the $Er_{0.57}Y_{0.43}Co_2$ deduced from the present investigation using different approaches. Column I shows T_c obtained from magnetization measurements (Sect. 3.1). In column II T_c is estimated from the temperature dependence of $\mu_{\rm Er}(T)$ by equation (2) (Fig. 4a). In columns III and IV, T_c is determined by the intersection of the tangent line $y'(T_0)$ and y_{min} (Eq. (1)) from the temperature dependences of the $\mu_{\rm Co}$ (Fig. 4b) and a (Fig. 3), respectively. The value for T_c, determined by neutron diffraction measurements in the way described above, is higher than the transition temperature derived from magnetization measurements, in agreement with earlier published data [6]. In contrast to the publication mentioned above [14], with $T_c^{\rm Co} = 11$ K, $T_c^{\rm Er} = 14.5$ K for ambient pressure and $p_{cr} < 3$ kbar for $Er_{0.6}Y_{0.4}Co_2$, we did not observe well separated magnetic transitions for the Er and the Co sublattice nor a collapse of the Co magnetic moment under a pressure of 6 kbar. Our recent neutron diffraction experiments on a $Er_{0.6}Y_{0.4}Co_2$ single-crystal under external magnetic fields up to 4 T also give direct evidence that the onset of long-range magnetic order for both magnetic sublattices occurs at about the same temperature [27]. These results qualitatively support a model of the magnetic state in these compounds in which the magnetization is associated with magnetic inhomogeneity (localized spin density fluctuations) of the sample owing to the statistical effects of the local environment [6,7]. Unlike to the first order transition in pure $ErCo_2$, the diluted compound has short-range magnetic order $\mu_{\rm Co} \neq 0$ (depending on the local Er-Y composition) even at $T > T_c$.

Table 3. The magnetic transition temperatures T_c [K] derived from magnetization and neutron diffraction measurements (see text).

p, kbar	I	II	III	IV
0	16.0(5)	20.0(9)	21.2(9)	19.2(9)
6.0(5)	13.4(5)	17.6(9)	17.4(9)	16.7(9)

5 Conclusion

The influence of external pressure on the magnetic structure near T_c has been studied for the cubic Laves-phase $Er_{0.57}Y_{0.43}Co_2$ by magnetization and neutron diffraction measurements. A formation of short-range magnetic order above T_c and a coexistence of short-range with long-range magnetic order from T_c down to $T = 4$ K is found. We established that (i) pressure decreases T_c approximately equally for both the Co and the Er sublattice; (ii) $\mu_{\rm Co}$ decreases with pressure unlike $\mu_{\rm Er}$, which remains constant up to 6 kbar. The multiple magnetic transitions reported previously could possibly be explained by sample segregation into yttrium-rich and yttrium-poor regions resulting in different (local) transition temperatures, or by some $(R_{1-x}Y_x)_nCo_m$ impurities known to exhibit a variety of transition temperatures.

We hope that our results contribute to a better understanding of the nature of the metamagnetic transition in these itinerant-electron systems and will stimulate further neutron scattering experiments under multiple (H, p) extreme conditions.

Financial support by the Swiss National Science Foundation (grant SCOPES No. 7 IP 65598) and Russian State Program "Neutron Investigation of Matter" (State contract No. 40. 012. 1. 1. 11. 50) is gratefully acknowledged.

References

1. E.P. Wohlfarth, P. Rhodes, Phil. Mag. **7**, 1817 (1962)
2. R.Z. Levitin, A.S. Markosyan, Sov. Phys. Usp. **31**, 730 (1988)
3. W. Steiner, E. Gratz, H. Ortbauer, H.W. Camen, J. Phys. F **8**, 1525 (1978)
4. N.V. Baranov, A.I. Kozlov, A.N. Pirogov, E.V. Sinitsyn, Sov. Phys. JETP **96**, 674 (1989)
5. N.V. Baranov, A.V. Andreev, H. Nakotte, F.R. de Boer, J.S.P. Klaasse, J. Alloys Comp. **182**, 171 (1992)
6. N.V. Baranov, A.N. Pirogov, J. Alloys Comp. **217**, 31 (1995)
7. N.V. Baranov, A.A. Yermakov, A.N. Pirogov, A.E. Teplykh, K. Inoue, Yu. Hosokoshi, Physica B **269**, 284 (1999)

8. R.Z. Levitin, A.S. Markosyan, V.V. Snegirev, Phys. Met. Metallogr. **57**, 56 (1984)
9. N.H. Duc, T.D. Hien, P.E. Brommer, J.J.M. Franse, J. Phys. F **18**, 275 (1988)
10. G. Hilscher, N. Pillmayr. C. Schmitzer, E. Gratz, Phys. Rev. B **37**, 3480 (1988)
11. Y. Nakamura, J. Magn. Magn. Mater. **31-34**, 829 (1983)
12. R. Hauser, C. Kussbach, R. Grössinger, G. Hilscher, Z. Arnold, J. Kamarád, A.S. Markosyan, E. Shappel, G. Chouteau, Physica B **294-295**, 182 (2001)
13. R. Hauser, R. Grössinger, G. Hilscher, Z. Arnold, J. Kamarád, A.S. Markosyan, J. Magn. Magn. Mater. **226-230**, 1159 (2001)
14. R. Hauser, E. Bauer, E. Gratz, M. Rotter, H. Michor, G. Hilscher, A.S. Markosyan, K. Kamishima, T. Goto, Phys. Rev. B **61**, 1198 (2000)
15. H. Yamada, M. Shimizu, Physica **161**, 179 (1989)
16. H. Yamada, J. Magn. Magn. Mater. **139**, 162 (1995)
17. R. Hauser, E. Bauer, E. Gratz, Phys. Rev. B **57**, 2904 (1998)
18. O. Syshchenko, T. Fujita, V. Sechovský, M. Divis, H. Fudjii, J. Magn. Magn. Mater. **226-230**, 1062 (2001)
19. O. Syshchenko, T. Fujita, V. Sechovský, M. Divis, H. Fudjii, Phys. Rev. B **63**, 054433 (2001)
20. E.F. Skelton, A.W. Webb, S.B. Qadri, S.A. Wolf, R.C. Lacoe, J.L. Feldman, W.T. Elam, E.R. Carpenter, C.Y. Huang, Rev. Sci. Instrum. **55**, 849 (1984)
21. P. Fischer, G. Frey, M. Koch, M.Könnecke, V. Pomjakushin, J. Schefer, R. Thut, N. Schlumpf, R. Bürge, U. Greuter, S. Bondt, E. Berruyer, Physica B **276-278**, 146 (2000)
22. J. Rodriguez-Carvajal, Physica B **192**, 55 (1993)
23. B. Bireckoven, J. Wittig, J. Phys. E **21**, 841 (1988)
24. S. Khmelevskyi, P. Mohn, J. Phys. Cond. Matt. **12**, 9453 (2000)
25. K. Ishiyama, A. Shinogi, K. Endo, J. Phys. Soc. Jpn **53**, 2456 (1984)
26. A. Pirogov, A. Podlesnyak, Th. Strässle, A. Mirmelstein, A. Teplykh, D. Morozov, A. Yermakov, to be published in Appl. Phys. A
27. A. Podlesnyak, Th. Strässle, J. Schefer, A. Furrer, A. Mirmelstein, A. Pirogov, P. Markin, N. Baranov, Phys. Rev. B **66**, 012409 (2002)